



## Research Paper

# Thermal, chemical and mechanical characterization of recycled corundum powder in metakaolin-based geopolymer binder

Giovanni Dal Poggetto<sup>a,\*</sup>, Marco Fortunato<sup>b</sup>, Anna Maria Cardinale<sup>b</sup>, Cristina Leonelli<sup>a,\*</sup>

<sup>a</sup> Department of Engineering "Enzo Ferrari", University of Modena and Reggio Emilia, Via P. Vivarelli 10, 41125 Modena, Italy

<sup>b</sup> DCCI- Department of Chemistry and Industrial Chemistry, University of Genoa, Via Dodecaneso 31, 16146 Genova (GE), Italy



## ARTICLE INFO

## Keywords:

Metakaolin  
Corundum  
Alkali activation  
Dehydroxylation  
Thermal analysis  
Waste

## ABSTRACT

In this study we report on the addition of a waste, a real spent corundum abrasive powder collected after testing, to a metakaolin-based alkali activated binder. The waste has been chosen as representative of spent grits produced by industrial blasting processes. In this model system based on metakaolin, the effect of corundum powder in the environment of high alkaline media was investigated in terms of 3D reticulation of the aluminosilicate amorphous structure of the consolidated geopolymeric mixes. A number of microstructural techniques (FT-IR, XRD, TGA/DTA) have been used in combination with less conventional one, such as the ionic conductivity measurements of the eluate produced after 24 h of immersion of the sample in water. The overall 3D aluminosilicate frame typical of MK-based geopolymer is retained also after 50 wt% addition of recycled corundum, as shown by FT-IR, XRD, and TGA/DTA. The traces of ceramic materials abrasion present in the waste showed good reactivity, as shown by the disappearance of their characteristic peaks in the XRD patterns. Ionic conductivity of the eluates evidenced the most extended reactivity of the alkaline activator solution in the case of 10 and 20 wt% addition of the waste. While the role of 20, 30 and 40 wt% addition of the waste to the MK-based matrix produced the highest compressive strength in the consolidated mortars after 28 days comparable to those of Ordinary Portland cement concretes. It was proved that, when produced using a partially reactive waste with well-formulated mix designs, metakaolin alkali-activated binders or mortars are an important aluminosilicate source for room temperature produced construction materials.

## 1. Introduction

Future trend in sustainable binders is agreed to be the substitution of alkali activated materials, AAMs, also indicated as geopolymers, to Ordinary Portland Cement, OPC [Mehta and Siddique, 2016; Komnitsas and Bartzas, 2021; Lolli and Kurtis, 2019]. Differently from OPC that requires high temperature clinker production, AAMs are produced via alkali activation of aluminosilicate powders that have already been thermally treated during their production, e.g. fly ash from coal-fired power station or metallurgical slags. Mineral raw materials are also used in AAMs formulations, e.g. kaolinitic and lateritic clay soils [Aldabsheh et al., 2015; Kaze et al., 2021], pozzolans [Barış and Tanacan, 2021], volcanic ash [Barone et al., 2021], requiring low temperature thermal treatments with respect to clinkerization. To reduce carbon footprint and increase sustainability, also the thermally treated minerals have been reduced in the binder mix [Sgarlata et al., 2022a] while the amount of reactive waste has been augmented [Alelweet and Pavia,

2019].

In the present study we approached the trend of increasing mix design sustainability for metakaolin (MK)-based geopolymers by inserting an increasing amount of a waste, abrasive corundum powder resulting from abrasion testing, up to 50 wt% (weight amounts based on dry matter). Corundum,  $\alpha$ -Al<sub>2</sub>O<sub>3</sub>, reduced in grains with particle size in the range of 0.01–300  $\mu$ m is a universal abrasive powder that finds wide technical application [Hacksteiner et al., 2018] and, at the same time, the spent abrasive powder represents a huge environmental problem [dos Anjos et al., 2017; Borucka-Lipska et al., 2019].

Differently from metakaolin, a metastable phase with stacking defects in the tetrahedral and octahedral sheets [Bellotto et al., 1995; Ortega et al., 2010], corundum crystalline grains are not easily solubilized in the majority of the alkali sources commonly used for the synthesis of geopolymers [Riahi et al., 2021], e.g. sodium hydroxides and sodium silicates as in the case under investigation.

The limited, though possible, dissolution process of corundum

\* Corresponding authors.

E-mail addresses: [giovanni.dalpoggetto@unimore.it](mailto:giovanni.dalpoggetto@unimore.it) (G. Dal Poggetto), [cristina.leonelli@unimore.it](mailto:cristina.leonelli@unimore.it) (C. Leonelli).

<https://doi.org/10.1016/j.clay.2023.106875>

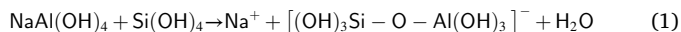
Received 5 September 2022; Received in revised form 6 February 2023; Accepted 20 February 2023

Available online 14 March 2023

0169-1317/© 2023 Published by Elsevier B.V.

particles when wetted by sodium hydroxide liquor, has been recorded as the presence of a diffusion layers of  $\text{NaAl}(\text{OH})_4$  around the corundum particles [Wu et al., 2016]. These Al-bearing species may foster the reaction with the  $\text{Si}(\text{OH})_4$  species coming from the metakaolin tetrahedral sheet or derived from the addition of soluble sodium silicate. Since the presence of soluble  $\text{Al}^{3+}$  ions in the dissolution step of the geopolymer formation results in a stronger 3D aluminosilicate network of the consolidated material [Garcia-Lodeiro et al., 2014], we expect that the addition of corundum grains to MK-based geopolymer could then act as filler with good matrix interface and induce positive influence on mechanical properties.

Concerning the consolidation step of the MK-based geopolymers, it has been widely reported that the reaction that take place is a condensation reaction occurring hopefully between soluble aluminium and silicon ions [Garcia-Lodeiro et al., 2014]:



The condensation can extend to the other -OH groups, till their complete elimination. The elimination of condensation water occurs via simple evaporation of the water from the sample surface without any evident shrinkage of the sample [corresponding to Region I in the description of Duxson et al., 2007]. The free water molecules remaining entrapped in the interconnect pores can be evaporated via thermal treatment in a temperature range approximately inferior to 220 °C [Rahier et al., 1996; Duxson et al., 2007; Tossell, 1999]. This thermal event, dehydration, corresponding to Region II [Duxson et al., 2007], can cause a reduced shrinkage from 4 to about 6%. Secondly, the loss of unreacted -OH groups, dehydroxylation, can be observed only at temperatures as high as 600–800 °C, that has been defined as Region III in MK-based geopolymers [Duxson et al., 2007]. Such a thermal event is characterised by gradual weight loss combined with thermal shrinkage, both processes requiring high temperature to occur. The dependence of the condensation steps is strictly related to the crystalline nature and chemical composition of the aluminosilicate powders used as precursors, as well as their mineralogy, finesses and chemical stability in alkaline media.

In conclusion, we can say that a number of properties are modified by the addition of a waste to the geopolymeric binder [Bahraq et al., 2020], and for the first time we investigated those produced by spent corundum grit. The valorisation of this type of waste in an inert matrix such as that created by MK-based geopolymer is also supported by another peculiarity of such material which is suitable to encapsulate different types of heavy metal cations as well as several anions if not macromolecules which might be present as contaminants of the waste [Komnitsas et al., 2013; Rooses et al., 2013; Sgarlata et al., 2022b]. Hereafter, we present the chemical and structural changes introduced by addition of abrasive corundum powders as collected after use to MK-based geopolymer formulations. A deep understanding of the microstructural and mechanical properties modifications due to the addition of the RC to the metakaolin, needs to be supported by a characterization as complete as possible, also depending on the future possible uses. As the characterization, we analysed the final consolidated materials reduced to powders by means of FT-IR, XRD, to check the structure modification and by TGA/DTA to evaluate the thermal stability [Cardinale et al., 2022]. To complete the study, some properties of bulky specimens (ionic conductivity of the eluate, compressive resistance) have been tested.

## 2. Materials and methods

### 2.1. Materials

The metakaolin (MK) used in this study was ARGICAL™ M1000 (Imerys S.A., Paris, France, chemical composition reported by the producer is reported in Table 1:  $\text{SiO}_2 = 55$ ;  $\text{Al}_2\text{O}_3 = 40$ ,  $\text{Fe}_2\text{O}_3 = 1.4$ ;  $\text{TiO}_2 = 1.5$ ;  $\text{Na}_2\text{O} + \text{K}_2\text{O} = 0.8$ ;  $\text{CaO} + \text{MgO} = 0.3$ ; and  $\text{LOI} = 1$  (wt%). We

**Table 1**

Mix proportion of geopolymers with RC. L is liquid (NaOH+Nasilicate), S is solid (MK + RC).

Mix ID	Weight %					H2O
	MK	RC	NaOH 8 M	Na-silicate solution	L/S	
GP0	100 (g)	0	38 (g)	40 (g)	7.8	32
90GP0-10RC	51	10	19	20	6.4	28
80GP0-20RC	45	20	17	18	5.4	25
70GP0-30RC	39	30	15	16	4.5	22
60GP0-40RC	34	40	12	14	3.5	19
50GP0-50RC	28	50	11	11	2.8	16

chose to use this type of aluminosilicate precursor because of its high reactivity, due to its fine particle size ( $D_{50} = 8.2 \mu\text{m}$ ;  $D_{90} = 33 \mu\text{m}$ ) and high surface area (B.E.T. =  $17 \text{ m}^2/\text{g}$ ) [Dal Poggetto et al., 2022] and appropriate molar Si/Al of 1.17, to be compare to pure MK with Si/Al = 1. Additionally, its use in literature as reference material for the geopolymer binders is very diffused [Moutinho et al., 2020].

The recycled corundum (RC) powder used in this study is the abrasive waste powder resulting from abrasion testing of different types of materials such as metals, ceramics, natural stones etc. It has an average particle size of about  $230 \mu\text{m}$  ( $D_{50} = 232 \mu\text{m}$ ) and it is composed of pure corundum,  $\text{Al}_2\text{O}_3$ , phase (92 wt%) with traces of ceramics and metallic powders for the remaining 8 wt%, as reported in a previous work [Dal Poggetto et al., 2022]. This type of waste is considered inert according to the regulation in force in Europe [Directive 2008/98/EC, 2023]. The NaOH solution was prepared by dissolving laboratory-grade granules (96 wt%, Sigma Aldrich, Italy) into distilled water to reach 8 mol/l (M, molarity) concentration. The sodium silicate solution ( $\text{SiO}_2/\text{Na}_2\text{O} = 3.00$  M ratio;  $\text{SiO}_2 = 26.50$  wt%,  $\text{Na}_2\text{O} = 8.70$  wt% and  $\text{pH} = 11.7$ ) with density of  $1.34 \text{ g}/\text{cm}^3$  at 20 °C was used in the formulation of the geopolymers in combination with NaOH. The solution of sodium silicate was supplied by Ingessil, Verona, Italy.

### 2.2. Preparation of geopolymer specimens

The reference geopolymer, hereafter indicated as GP0, was obtained by adding 38 g of NaOH, 8 M plus 40 g of sodium silicate solution to the amount of 100 g of MK, dry powder, under mechanical stirring, as optimised in a previous work [Dal Poggetto et al., 2022]. After the GP0 fresh paste preparation, addition of the as-received recycled corundum powder in the amounts of 10, 20, 30, 40 and 50 wt% (percentage of RC have been calculated with respect to the total mass of the composite formulation in the wet status) was performed to produce the geopolymer composites labelled 90GP-10RC, 80GP-20RC, 70GP0-30RC, 60GP0-40RC and 50GP0-50RC, respectively, as indicated in Table 1. Amounts of RC higher than 50 wt% compromised the workability of the mix. The formulations maintained constant the MK/NaOH and MK/silicate weight ratio in the different composites. All formulations were mixed in a Planetary Mixer (Aucma 1400 W, China) then poured into silicone cubic moulds ( $25 \text{ mm} \times 25 \text{ mm} \times 25 \text{ mm}$ ). Before closing the samples and letting them rest for 28 days at room temperature, the bubbles were removed with the shaking table. Typically, geopolymer binders are compared to Ordinary Portland cement products, hence we chose the 28 days curing/ageing time to have better comparability with literature data (See Section: 3.4 Mechanical properties).

### 2.3. Geopolymers characterization

The consolidated materials were tested at 28 days of ageing time

either in the form of powders (FT-IR, TGA/DTA, XRD) as well as in the form of bulk solids (ionic conductivity of the eluate, compressive resistance) with the aim to evidence the effect of RC addition on the nano and microscale as well as on the macroscale properties of the final composites.

### 2.3.1. Spectroscopic characterization

One of the characterization techniques most sensitive to the features of aluminosilicate chemical bonds is Fourier Transform Infra-Red spectroscopy. Several studies have been already published for the interpretation of MK based geopolymers [Catauro et al., 2020].

FT-IR analysis (Prestige21 Shimadzu spectrophotometer, Shimadzu Italia s.r.l., Milano, Italy, equipped with a detector deuterated triglycine sulphate with potassium bromide windows) were carried out on the geopolymers with and without RC with the aim of observing the presence of Al in the lattice of the geopolymers with RC. The analysis was performed in the spectral region of 400–4000  $\text{cm}^{-1}$  and with a resolution of 2  $\text{cm}^{-1}$  (60 scans). For the analysis, KBr disks containing 2 mg of sample and 198 mg of KBr were used. FT-IR spectra were elaborated by IRsolution as well as Origin 9 software packages.

### 2.3.2. Thermal characterization

Differential thermal analysis-thermo-gravimetry (TGA/DTA) was performed using a LabsysEvo 1600–Setaram apparatus (Setaram, Calurie, France) with a double thermocouple Platinum/Platinum-Rhodium 10%, the thermocouples were calibrated by using, as calibration materials, high-purity elements such as Ag, Au. About 30 mg of powdered sample were placed in an open alumina crucible and heated from 30 °C to 1250 °C at 10 °C/min under argon flux (60  $\text{mL min}^{-1}$ ); due to the origin of the sample (waste), which could be affected by impurities, the measurements were carried out under inert atmosphere, to avoid side reactions. In the temperature range considered, the error on mass loss determination was 0.2% and in temperature determination 0.5%.

### 2.3.3. Mineralogical composition

Crystalline phases of the geopolymers and raw materials (MK and RC) were identified on powdered specimens via X-ray diffraction (XRD) (X'Pert PRO, PANalytical, Malvern Panalytical Ltd., Malvern, UK). The diffractometer was operated at 40 kV and 40 mA using Cu-K $\alpha$  radiation (Ni filtered). Diffraction patterns were collected by the X'Celerator detector from 5 to 70° 2 $\theta$  with a step size of 0.02° 2 $\theta$  and a counting time of 3 s, slit width 10. It should be noted that the as-received waste corundum powder was not finely ground to avoid contamination from milling media as it is an extremely hard abrasive (value of 9 on the Mohs hardness scale). Mineral phases were identified by comparing the experimental peaks with reference patterns (DIFFRAC plus EVA software, 2005 PDF2, Bruker, Billerica, MA, USA). Preferential orientation was avoided by side charging the powdered specimen.

### 2.3.4. Ionic conductivity of eluates

The chemical stability of the 3D aluminosilicate network reticulated within the geopolymer final products was evaluated through immersion in distilled water (Milli-Q® Lab Water) of bulky cubic specimens (liquid to solid ratio = 1/10) and ionic conductivity measurements on the eluate solutions [Dal Poggetto et al., 2022]. Ionic conductivity measurements of such solutions were performed with Crison GLP31 (Hach Lange Spain, S.L.U, Barcelona, Spain) and compared them with the ionic conductivity of Milli-Q water (0.2  $\text{mS/m}$ ).

### 2.3.5. Mechanical properties

Mechanical performance of the cubic specimens was tested under compression in an Instron 5567 Universal Testing Machine after 28 days of curing. The load (30 kN load limit) was applied and increased by displacement rate of 1 mm/min. Compressive strength values are given as the mean value of eight tests accompanied with the 2% variance.

### 2.3.6. SEM

Microstructure observations were conducted by ESEM (ESEM-Quanta200-FEI) equipped with EDS to evaluate both the formation of geopolymeric amorphous phase and the presence of unreacted particles of corundum and aluminosilicate in the hardened samples after 28 days of curing. Before SEM analysis the freshly fractured surface of each specimen was coated with an Au sputtered layer.

## 3. Results

### 3.1. Spectroscopic characterization

FT-IR spectra of MK and geopolymers with RC at 28 days of curing time are reported in Fig. S1 (see Supplementary Materials) and indicate that the addition of RC at any percentage does not alter the reticulation of metakaolin after alkali activation. In the MK spectrum the bands at 3440  $\text{cm}^{-1}$  and 1640  $\text{cm}^{-1}$  are assigned to –OH stretching and bending vibration of water's hydration [Catauro et al., 2016; Tchakouté et al., 2016]. The band at 1077  $\text{cm}^{-1}$  is assigned to Si–O–Si or Si–O–Al asymmetric stretching vibrations [Catauro et al., 2020]. Indeed, this band shifts to a lower wavenumber (1018–1011  $\text{cm}^{-1}$ ) for all the geopolymers, with and without RC, suggesting the increase in the number of Si–O–Al bonds, it also means that the geopolymerization took place regularly like all MK-based geopolymer. With the addition of recycled corundum, the percentage of Al which could bond with Si increases, yet a relevant shift of this band towards lower wavelength numbers cannot be assessed. The Si–O bands observed at 800 and 460  $\text{cm}^{-1}$  indicate the presence of quartz [Tchakouté et al., 2016] (see also XRD patterns in Fig. 3). The absorption band at 560  $\text{cm}^{-1}$  could be related to the existence of Al–O vibrations of Al in six-fold coordination [Krishna Priya et al., 1997; Tchakouté et al., 2016], due to the presence of traces of illite in MK [Panias et al., 2007; Tchakouté et al., 2016].

### 3.2. Thermal characterization

All the samples under investigation show a similar behaviour during the TGA/DTA analysis, losing mass in one single step attributable to the evolution of free water combined plus water coming from the dehydroxylation step, as presented in similar composition as reported in literature by [Duxson et al., 2007] for samples with similar composition, The TGA/DTA patterns for all the samples are reported in the supplementary data (Fig. S2).

A comparison of the TGA curves, among all the different samples under investigation, is shown in Fig. 1a), while in Fig. 1b) is graphically describing the relationship between the mass decrease under heating and the composition of the sample. Fig. 1a) reveals that the starting point of the mass losses seems not to be influenced by the different amount of RC added to the mixture, and from Fig. 1b) turns out clearly the inverse linear correlation between the mass loss and the percentage of corundum in the sample. Moreover, from Fig. 2a) also the heat flow involved in the dehydration of the different samples increases in a regular way by increasing the amount of GP0 in the mixture, and the relation between the GP0 percentage and the heat flow (calculated by the integral area of the curve in Fig. 2a) (Fig. 2b) is linear again, decreasing with the percentage of RC added. The mass losses of the two samples GP0 and 50GP0 differ by about 50% Finally, both processes (the mass loss and the heat flow) follow a linear trend, suggesting that there is no chemical interaction between the geopolymer and the recycled corundum.

### 3.3. Mineralogical composition

The diffraction pattern collected on the pulverised GP0 sample (Fig. 3) shows the typical diffuse reflection of the amorphous aluminosilicate structure plus sharper peaks identified as anatase, TiO<sub>2</sub>, and alpha-quartz,  $\alpha$ -SiO<sub>2</sub>, present in the metakaolin. Original crystalline

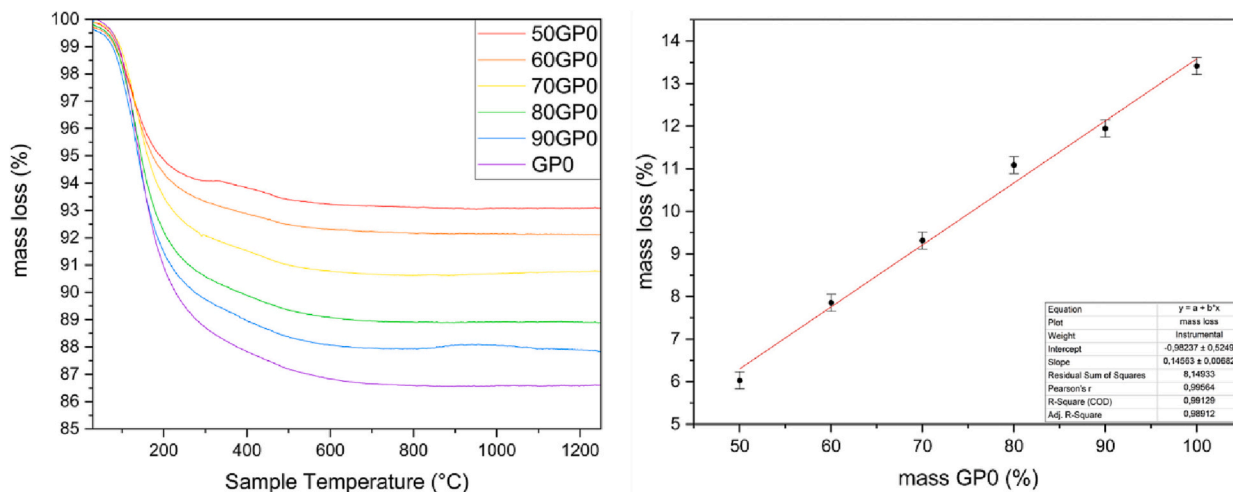


Fig. 1. a) TGA curves for the different samples, b) mass loss (mass%) vs sample composition.

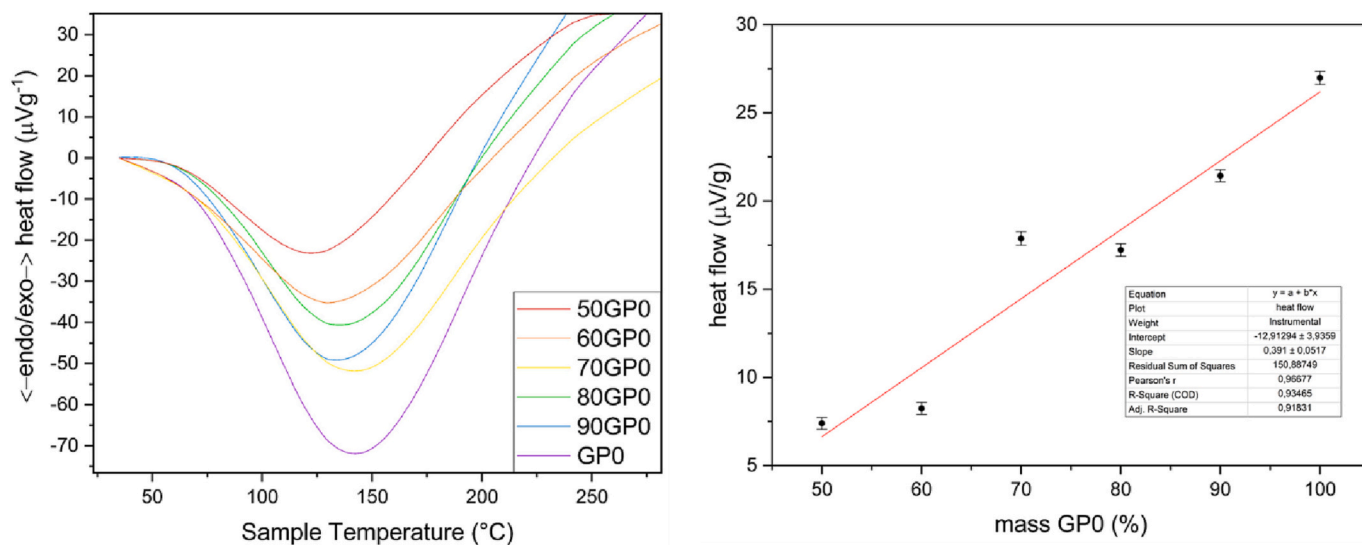


Fig. 2. a) heat flow involved during heating in the mass loss temperature range; b) heat involved (heat flow) vs sample composition.

structure of kaolinite,  $\text{Al}_2\text{Si}_2\text{O}_5(\text{OH})_4$ , at around  $20^\circ$  in  $2\theta$ , is present in the as-received MK and it is visible in all the patterns with the exception of 50GP-50RC containing the lower amount of MK [Gasparini et al., 2013]. Anatase, a MK impurity, is present with one peak that disappears when the MK percentage decreases in the formulation starting from 80GP0-20RC (this pattern has been enlarged in y-axis). The diffraction patterns collected from 90GP0-10RC to 60GP0-40RC are similar, and all have a diffuse reflections characteristic of amorphous geopolymer at about  $26\text{--}28^\circ$  in  $2\theta$  [Temuujin et al., 2009; Catauro et al., 2020]. With the addition of the RC, the typical corundum,  $\alpha\text{-Al}_2\text{O}_3$  peaks begin to be noticed, which increase in intensity with the increase of the percentage of RC. It is also possible to note that in the spectra from 90GP0 to 60GP0 there are no peaks at  $8^\circ$  and  $16^\circ$  in  $2\theta$  due to the impurities present in the recycled corundum, namely montmorillonite,  $(\text{Na,Ca})_{0.3}(\text{Al,Mg})_2\text{Si}_4\text{O}_{10}(\text{OH})_2 \cdot n(\text{H}_2\text{O})$ , and analcime,  $\text{NaAlSi}_2\text{O}_6 \cdot (\text{H}_2\text{O})$ . This means that the environment is basic enough for the impurities present in the RC to react as well. The amorphous hump shifts in the XRD patterns confirm the Si-O-Si to Si-O-Al network of the amorphous fraction of the geopolymeric samples. In Fig. 3 it can also be seen that the diffraction of the 50GP0-50RC sample shows the peaks of the impurities of the recycled corundum (both these patterns have been enlarged in y-axis), indicating that these crystalline phases have not been dissolved in the alkaline

media added as activator for metakaolin.

#### 3.4. Ionic conductivity of eluate

The water immersion test evaluates the chemical stability of the 3D aluminosilicate network of the geopolymers, as reported by recent literature [Sánchez Díaz and Escobar Barrios, 2022]. The ionic conductivity of the solutions obtained after the immersion in water of geopolymer specimens increases as a consequence of unreacted alkaline solution leaching out. The higher is the unreacted fraction of the alkaline activator, the higher the ionic conductivity of the eluate.

It can be noted in Fig. S3 (see Supplementary Materials) that the difference between GP0 and the geopolymer is relevant for the formulations from 90GP0-10RC to 60GP-40RC, while the formulation with 50 wt% of RC is closer to GP0. After 24 h of immersion, all the formulations reach a constant value being for the 10 and 20 wt% addition of RC very similar, while scarcely increasing for 30 and 40 wt% (Fig. 4). Samples showing lowest ionic conductivity, 90GP0-10RC and 80GP0-20RC, corresponding to the better reticulated MK-geopolymeric matrix, are also the formulations showing highest mechanical strength (see comments to Fig. 4).

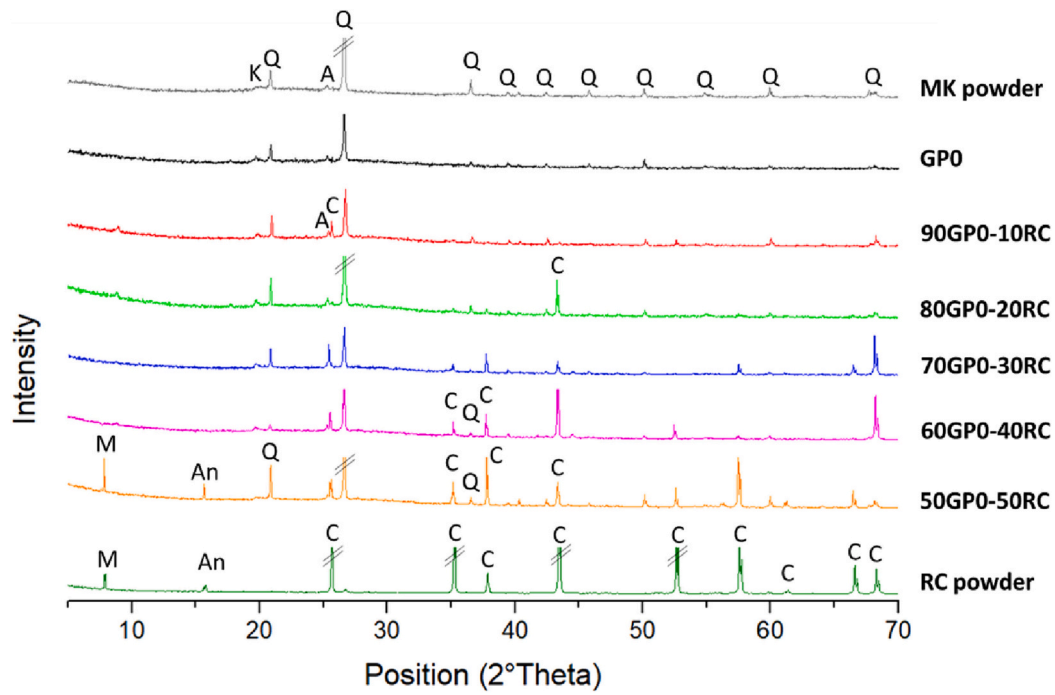


Fig. 3. XRD patterns for MK powder, GP0, 90GP0-10RC, 80GP0-20RC\*, 70GP0-30RC, 60GP0-40RC, 50GP0-50RC\* and Recycled Corundum\* powder. Crystalline phases identification label: Q = Quartz, K = Kaolinite, A = Anatase, M = Montmorillonite, An = Analcime and C = Corundum. \*Larger Y-axis scale.

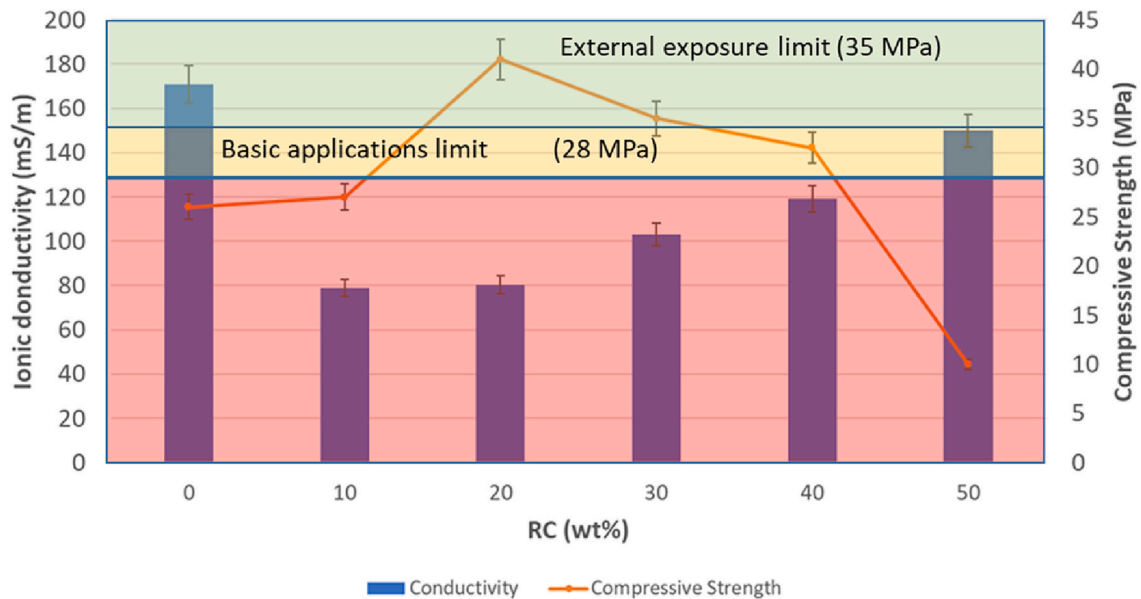


Fig. 4. Compressive strength correlated with the ionic conductivity of the leachate solution after 24 h of immersion time, i.e. when the measurements recorded a constant number. All the samples after 28 days are correlated with values of Table 2.

3.5. Mechanical properties

The compressive strength tests were performed after 28 days of curing on all the geopolymer samples. According to ACI 318 M-05 [ACI M318-05 2005, 2005], the 28-d compressive strength of concrete need to achieve at least 28 MPa for the basic engineering application (Table 2). For the corrosion protection of reinforcement in concrete, the minimum compressive strength of concrete is 35 MPa. In the present study, the presence of corundum powder can be resembled to the presence of fine aggregates, or sand, in a mortar. So, we can assume that our mixes are close to those of binders based on Ordinary Portland

Table 2

Requirements for special exposure conditions for concrete [ACI M318-05 2005, 2005].

Exposure Condition	Minimum Mpa
Low permeability when exposed to water	28
Exposure to freezing and thawing in humid conditions or deicing chemicals	31
Sulfate Exposure	28-31
Exposure to chlorides from deicing chemicals, salt, salt water, brackish water, seawater	35

cement added with fine aggregates, even though in our case the percentage of RC is lower than 50 wt%. Additionally, the values we are using as comparison from Table 2 are referred to concretes, a mixture with fine and coarse aggregates. We are not processing concrete, i.e. we are not adding coarse aggregates that notably increase compression resistance, nevertheless, the strength developed by our materials is significantly high to be comparable to those of concrete.

From Fig. 4 it is possible to notice that after an addition of 10% by weight of recycled corundum the value does not change particularly with respect to GP0 formulation. The situation is different by adding 20 wt% of the waste corundum, as the compressive strength greatly increases. After the addition of 30 and 40 wt% the values are still good, yet

already decreasing. Indeed, the 50GP0-50RC formulation shows the worst compressive strength. For samples 60GP0-40RC as well as for 50GP0-50RC the compactness of the bulk materials decreases, exposing the matrix to higher amounts of water with increased ions leaching (Fig. 4).

The correlation between strength and porosity was proved to be poorly dependent on concrete composition [Kronlöf, 1994; Chuah et al., 2016]. With increasing the RC content, the amount of geopolymeric paste of formulation GP0 was decreased till a point (corresponding to about 20–25% of RC calculated on RC + MK powders) when the porosity starts to become an unfavourable factor weakening the mechanical strength of the final consolidated material. The paste to inert filler

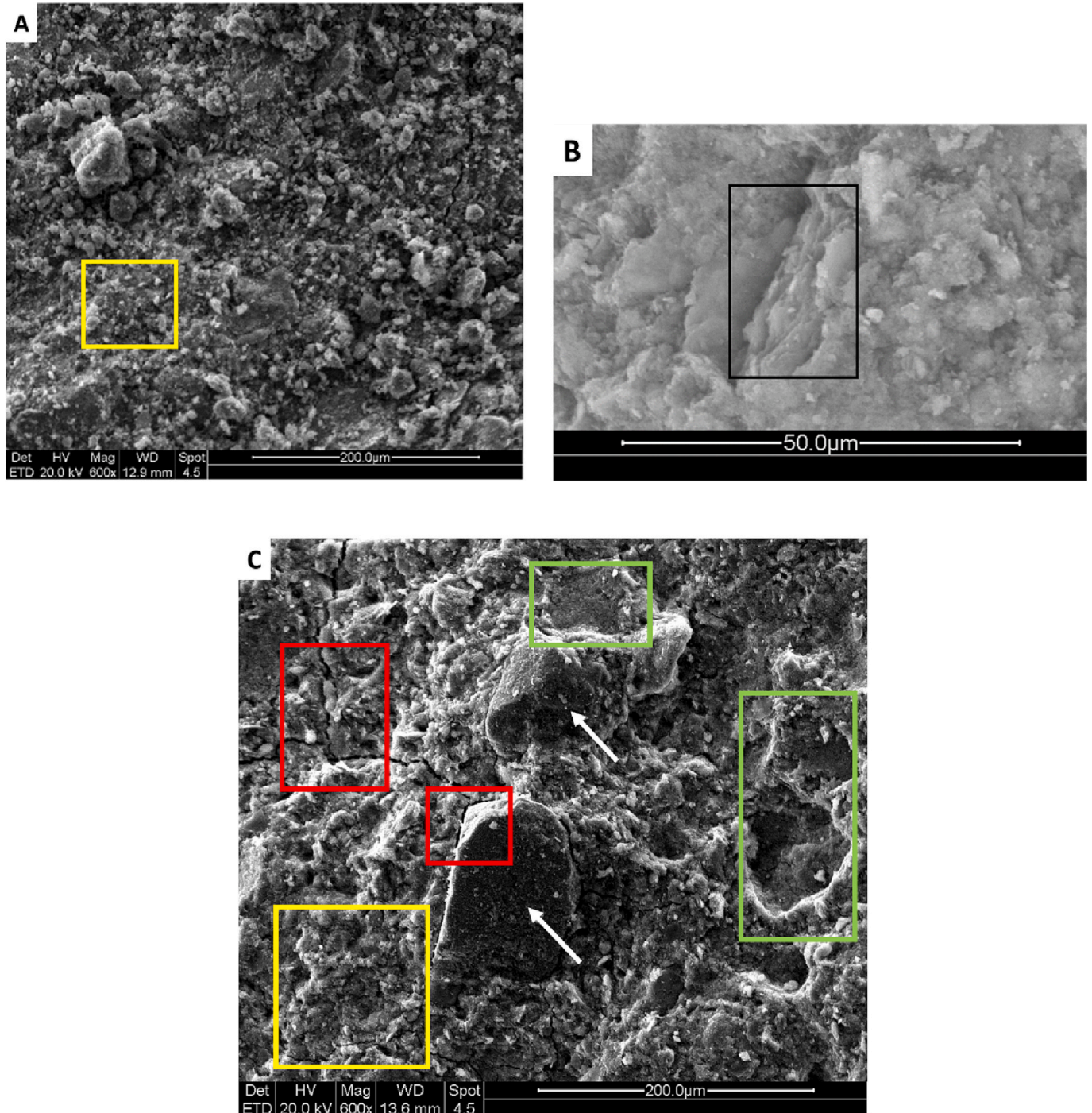


Fig. 5. Scanning Electron Microscopy images taken at low magnification (600 $\times$ ) to evidence the different toughening mechanics: a-b) GP0 and c) 90GP0-10RC.

interaction was proved to improve by both compactness of the water-binder suspension around the aggregate particles and the total interface area, which increases with aggregate fineness. Thanks to these two mechanisms the use of finer RC fillers will prove to have a more remarkable strengthening effect than the grain size used in this investigation.

### 3.6. SEM

SEM observations evidenced the presence of a very dense microstructure (yellow area in Fig. 5) where the recycled corundum irregular grains are embedded in the geopolymeric network. The maps of each single element (Al, Si, Na, O) have not been useful in depicting specific microstructures since the distribution is uniform in the matrix of geopolymer. From the maps it was possible to localize the RC grains (Fig. 5, c). Additionally, the SEM images at high enlargements are equally not significant showing the dense geopolymeric gel (see Fig. 5,b). Differently from some unreacted MK lamellar particles (enlarged black area, Fig. 5,b), the remaining aluminosilicate powder is fully reacted, showing the typical spongy-like geopolymeric structure (Fig. 5,a). When RC is added, its distribution was found to be homogenous within the geopolymeric matrix. At low magnification, the crack deflection mechanism (red area in Fig. 5) can be observed together with pull-out (green area in Fig. 5). These two toughening mechanisms indicate that the interface between the RC grain and the matrix is weak due to low reactivity of the crystalline corundum surface. In the pull-out area it was possible to observe the densification of the matrix at the surface of the corundum particle (See also Figs. S4 to S7 in the Supplementary Materials for the other composites). This observation confirms that in each composition, the MK particles have fully reacted with the activator solution thank to the impervious surface of the corundum grain that did not absorb this solution.

## 4. Discussions

Comparing this study with a previous one [Dal Poggetto et al., 2022], some differences and similarities can be noted:

- Fast room temperature consolidation in both formulations, since after 24 h in plastic mould all geopolymers were demoulded without deformation. Furthermore, good chemical stability in air, as proved by the absence of efflorescence at the solid surface in all consolidated samples.
- In both studies the insertion of RC as precursor or filler slightly shifts the ionic conductivity of water from that of the reference GPO formulation: ionic conductivity increases from GPO to all formulations with RC. Moreover, the ionic conductivity presented in the published paper [Dal Poggetto et al., 2022] is higher than those presented in this study.
- The compressive strength of geopolymers prepared in the previous study [Dal Poggetto et al., 2022] decreases with the addition of RC, while in this study the compressive strength of geopolymers increases up to 50 wt% of RC.

## 5. Conclusions

With the aim to avoid landfilling or sub valorisation of spent abrasive powder, the present contribution proved that an uptake up to 50 wt% of waste corundum is possible within a matrix of metakaolin-based geopolymeric binder. The reactivity of the trace minerals contained in the as-received spent abrasive powder was proved by XRD diffraction, whilst FT-IR reported a stable 3D aluminosilicate network with increasing RC content. Thermal decomposition proved that the role of corundum does not affect the overall reticulation process of the metakaolin based matrix presenting linear mass loss as well as linear dehydroxylation energy trends with increasing RC content. The ionic

conductivity of the eluate after 24 h of immersion of the sample in water was proved to be a more sensitive technique to investigate microstructure than the previous ones. Such a measurement indirectly evidences the amount of unreacted ionic species still present in the consolidated product, being the addition of 10 or 20 wt% of RC (90GPO-10RC or 80GPO-20RC) efficiently capable of reducing the ionic conductivity. The potential use of the consolidated product as sustainable construction material was proved by means of compressive resistance testing at 28-days of ageing. Even though the mixes presented here can be described as mortars, the mechanical resistance is comparable (up to 50GPO-50RC formulation) to that of concrete produced using Ordinary Portland cement.

It has been possible to evidence how the geopolymer composites consolidated after the addition of RC are comparable to Ordinary Portland concrete, as far the mechanical resistance to compression is concerned, and are almost all suitable for exposure to sulphates. We are confident that after the addition of also the prescribed amount of coarse aggregates to our formulations, as required for concrete, the mechanical properties could increase and reach the values requested for concrete to be used in special exposure conditions.

Future investigations in the direction of less cost-effective aluminosilicate source with respect to metakaolin and particular consideration of the environmental footprint of the alkaline activator will be addressed.

### Funding sources

This research did not receive any specific grant from funding agencies in the public, commercial, or not-for-profit sectors.

### CRediT authorship contribution statement

**Giovanni Dal Poggetto:** Investigation, Data curation, Writing – original draft. **Marco Fortunato:** Data curation, Formal analysis. **Anna Maria Cardinale:** Methodology, Writing – review & editing. **Cristina Leonelli:** Supervision, Resources, Writing – original draft, Writing – review & editing.

### Declaration of Competing Interest

The authors declare that they have no known competing financial interests or personal relationships that could have appeared to influence the work reported in this paper.

### Data availability

Part of the original data supporting reported results are included in the Supplementary Materials. Further inquiries can be directed to the corresponding author.

### Acknowledgements

Authors are particularly grateful for metakaolin supply to Sophie Maraninchi, Product Manager Refractory, Abrasives and Constructions Business Area, Imerys, France, and Paola Morsiani, Sales Manager, Performance Minerals EMEA/Ceramics, Imerys Ceramics Italy. Authors express their gratitude to Dr. Mirko Braga, Ingessil, Montorio, Italy, for supplying the sodium silicate solution.

### Appendix A. Supplementary data

Supplementary data to this article can be found online at <https://doi.org/10.1016/j.clay.2023.106875>.

## References

- ACI M318–05 2005, 2005. ACI M318–05 Building Code Requirements for Structural Concrete and Commentary American Concrete Institute.
- Aldabsheh, I., Khoury, H., Wastiels, J., Rahier, H., 2015. Dissolution behavior of Jordanian clay-rich materials in alkaline solutions for alkali activation purpose. Part I. *Appl. Clay Sci.* 115, 238–247.
- Alelweat, O., Pavia, S., 2019. An evaluation of the feasibility of several industrial wastes and natural materials as precursors for the production of alkali activated materials. *World Acad. Sci. Eng. Technol.* 13 (12).
- Bahraq, A.A., Maslehuddin, M., Al-Dulaijan, S.U., 2020. Macro- and micro-properties of engineered cementitious composites (ECCs) incorporating industrial waste materials: a review. *Arab. J. Sci. Eng.* 45 (10), 7869–7895.
- Bariş, K.E., Tanaçan, L., 2021. Improving the geopolymeric reactivity of Earth of Datça as a natural pozzolan in developing green binder. *J. Build. Eng.* 41, 102760.
- Barone, G., Finocchiaro, C., Lancellotti, I., Leonelli, C., Mazzoleni, P., Sgarlata, C., Strosio, A., 2021. Potentiality of the use of pyroclastic volcanic residues in the production of alkali activated material. *Waste Biomass Valorization* 12 (2), 1075–1094.
- Bellotto, M., Gualtieri, A., Artioli, G., Clark, S.M., 1995. Kinetic study of the kaolinite-mullite reaction sequence. Part I: Kaolinite dihydroxylation. *Phys. Chem. Miner.* 22 (4), 207–217. <https://doi.org/10.1007/BF00202253>.
- Borucka-Lipska, J., Techman, M., Skibicki, S., 2019. Use of contaminated sand blasting grit for production of cement mortars. *IOP Conf. Ser. Mater. Sci. Eng.* 471 (3) <https://doi.org/10.1088/1757-899X/471/3/032055> art. no. 032055.
- Cardinale, A.M., Vecchio Cipriotti, S., Fortunato, M., Catauro, M., 2022. Thermal behavior and antibacterial studies of a carbonate Mg–Al-based layered double hydroxide (LDH) for in vivo uses. *J. Therm. Anal. Calorim.* <https://doi.org/10.1007/s10973-022-11334-3>.
- Catauro, M., Bollino, F., Cattaneo, A.S., Mustarelli, P., 2016. Al<sub>2</sub>O<sub>3</sub>·2SiO<sub>2</sub> powders synthesized via sol–gel as pure raw material in geopolymer preparation. *J. Am. Ceram. Soc.* 100, 1919–1927.
- Catauro, M., Dal Poggetto, G., Sgarlata, C., Vecchio Cipriotti, S., Pacifico, S., Leonelli, C., 2020. Thermal and microbiological performance of metakaolin-based geopolymers cement with waste glass. *Appl. Clay Sci.* 197, 105763.
- Chuah, S., Duan, W.H., Pan, Z., Hunter, E., Korayem, A.H., Zhao, X.L., Collins, F., Sanjayam, J.G., 2016. The properties of fly ash based geopolymer mortars made with dune sand. *Mater. Des.* 92, 571–578.
- Dal Poggetto, G., D'Angelo, A., Catauro, M., Barbieri, L., Leonelli, C., 2022. Recycling of waste corundum abrasive powder in MK-based geopolymers. *Polymers* 14 (11), 2173.
- Directive 2008/98/EC, 2023. <https://eur-lex.europa.eu/eli/dir/2008/98/oj>.
- dos Anjos, M.A.G., Sales, A.T.C., Andrade, N., 2017. Blasted copper slag as fine aggregate in Portland cement concrete. *J. Environ. Manag.* 196, 607–613. <https://doi.org/10.1016/j.jenvman.2017.03.032>.
- Duxson, P., Lukey, G.C., Van Deventer, J.S.J., 2007. Physical evolution of Na-geopolymer derived from metakaolin up to 1000 °C. *J. Mater. Sci.* 42 (9), 3044–3054.
- García-Lodeiro, I., Palomo, A., Fernández-Jiménez, A., 2014. An overview of the chemistry of alkali-activated cement-based binders, Chapter 2. In: Pacheco-Torgal, F., Labrincha, J.A., Leonelli, C., Palomo, A., Chindaprasit, P. (Eds.), *Handbook of Alkali-Activated Cements, Mortars and Concretes*. Publisher: Elsevier Inc./ Woodhead Publishing Series in Civil and Structural Engineering, pp. 19–47, 1st Edition - November 3, 2014, ISBN: 978-178242288-4, 978-178242276-1.
- Gasparini, E., Tarantino, S.C., Ghigna, P., Cedillo-Gonzalez, E.I., Siligardi, C., Zema, M., 2013. Thermal dihydroxylation of kaolinite under isothermal conditions. *Appl. Clay Sci.* 80–81, 417–425.
- Hacksteiner, M., Peherstorfer, H., Bleicher, F., 2018. Energy efficiency of state-of-the-art grinding processes. *Procedia Manuf.* 21, 717–724.
- Kaze, C.R., Adesina, A., Lecomte-Nana, G.L., Alomayri, T., Kamseu, E., Melo, U.C., 2021. Alkali-activated laterite binders: influence of silica modulus on setting time, rheological behaviour and strength development. *Clean. Eng. Technol.* 4, 100175.
- Komnitsas, K.A., Bartzas, G., 2021. Editorial for special issue: alkali activated materials: advances, innovations, future trends. *Minerals* 11 (1), 75.
- Komnitsas, K., Zaharaki, D., Bartzas, G., 2013. Effect of sulphate and nitrate anions on heavy metal immobilisation in ferronickel slag geopolymers. *Appl. Clay Sci.* 73, 103–109. <https://doi.org/10.1016/j.clay.2012.09.018>.
- Krishna Priya, G., Padmaja, P., Warriar, K.G.K., Damodaran, A.D., Aruldas, G., 1997. Dehydroxylation and high temperature phase formation in sol-gel boehmite characterized by Fourier transform infrared spectroscopy. *J. Mater. Sci. Lett.* 16 (19), 1584–1587.
- Kronlóf, A., 1994. Effect of very fine aggregate on concrete strength. *Mater. Struct.* 27, 15–25.
- Lolli, F., Kurtis, K.E., 2019. Life Cycle Assessment of alkali activated materials for pavement applications: preliminary investigation of precursors. *RILEM Tech. Lett.* 6, 124–130.
- Mehta, A., Siddique, R., 2016. An overview of geopolymers derived from industrial, by-products. *Constr. Build. Mater.* 127, 183–198.
- Moutinho, S., Costa, C., Andrejkovicova, S., Mariz, L., Sequeira, C., Terroso, D., Rocha, F., Velosa, A., 2020. Assessment of proper-ties of metakaolin-based geopolymers applied in the conservation of tile facades. *Constr. Build. Mater.* 259, 119759.
- Ortega, A., Macías, M., Gotor, F.J., 2010. The multistep nature of the kaolinite dehydroxylation: Kinetics and mechanism. *J. Am. Ceram. Soc.* 93 (1), 197–203.
- Panias, D., Giannopoulou, I.P., Perraki, T., 2007. Effect of synthesis parameters on the mechanical properties of fly ash-based geopolymers. *Colloids Surf. A Physicochem. Eng. Asp.* 301, 246–254.
- Rahier, H., Van Mele, B., Wastiels, 1996. Low-temperature synthesized aluminosilicate glasses: part II. Rheological transformations during low-temperature cure and high-temperature properties of a model compound. *J. Mater. Sci.* 31 (1), 80.
- Riahi, S., Nemat, A., Khodabandeh, A.R., Baghshahi, S., 2021. Investigation of interfacial and mechanical properties of alumina-coated steel fiber reinforced geopolymer composites. *Constr. Build. Mater.* 288, 123118.
- Rooses, A., Steins, P., Dannoux-Papin, A., Lambertin, D., Poulesquen, A., Frizon, F., 2013. Encapsulation of Mg–Zr alloy in metakaolin-based geopolymer. *Appl. Clay Sci.* 73, 86–92.
- Sánchez Díaz, E.E., Escobar Barrios, V.A., 2022. Development and use of geopolymers for energy conversion: an overview. *Constr. Build. Mater.* 315, 125774.
- Sgarlata, C., Formia, A., Siligardi, C., Ferrari, F., Leonelli, C., 2022a. Mine clay washing residues as a source for alkali-activated binders. *Materials* 15, 83. <https://doi.org/10.3390/ma15010083>.
- Sgarlata, C., Leonelli, C., Lancellotti, I., Mortalò, C., Berrettoni, M., Fattobene, M., Zamponi, S., Giorgetti, M., 2022b. Sustainable chromium encapsulation: alkali activation route. *Front. Mater.* 9.
- Tchakouté, H.K., Rüscher, C., Kong, S., Kamseu, E., Leonelli, C., 2016. Geopolymer binders from metakaolin using sodium waterglass from waste glass and rice husk ash as alternative activators: a comparative study. *Constr. Build. Mater.* 114, 276–289.
- Temuujin, J., Minjigmaa, A., Rickard, W., Lee, M., Williams, L., Riessen, A.V., 2009. Preparation of metakaolin based geopolymer coatings on metal substrates as thermal barriers. *Appl. Clay Sci.* 46, 265–270.
- Tossell, J.A., 1999. Theoretical studies on aluminate and sodium aluminate species in models for aqueous solution: Al(OH)<sub>3</sub>, Al(OH)<sub>4</sub><sup>-</sup>, and NaAl(OH)<sub>4</sub>. *Am. Mineral.* 84, 1641–1649.
- Wu, Yu-Sheng, Li, Hong-Liang, Shi, Feng-Ling, Liu, Xiao-Fu, Su, Gui-Qao, Qu, Yan-Ping, 2016. Corundum dissolution in concentrated sodium hydroxide solution. *China Found. Res. Dev.* 13 (6), 422–426. <https://doi.org/10.1007/s41230-016-5064-4>.